PERFORMANCE OF LOW-ENERGY MAGNETIC BUNCH COMPRESSION FOR THE ASTA PHOTOINJECTOR AT FERMILAB*

C.R. Prokop, Department of Physics, Northern Illinois University DeKalb, IL 60115, USA
P. Piot, Department of Physics, Northern Illinois University DeKalb, IL 60115, USA
and Fermi National Accelerator Laboratory, Batavia, IL 60510, USA
B.E. Carlsten, Los Alamos National Laboratory, Los Alamos, NM, 87544 USA
M. Church, Fermi National Accelerator Laboratory, Batavia, IL 60510, USA

Abstract

The Advanced Superconducting Test Accelerator (ASTA) at Fermilab incorporates a magnetic bunch compressor chicane to compress the 40-MeV electron bunches generated in the photoinjector. In this paper, we present a numerical analysis and parametric study of the bunch compressor's performance for various operating scenarios. The beam dynamics simulations, carried out with IMPACT-Z and CSRTRACK, are compared against each other. Finally an operating regime with minimal phase space dilutions is suggested based on the simulation results.

INTRODUCTION

The Advanced Superconducting Test Accelerator (ASTA) at Fermilab is a superconducting linear electron accelerator currently under construction is planned to support a variety of user and Advanced Accelerator R&D (AARD) experiments [1, 2]. The facility's construction is staged and the initial phase, which will support first beam operation, consists of a photoinjector and one accelerating cryomodule [3].

In this paper, we consider the beamline detailed in Fig. 1 which details the photoinjector. In this photoinjector the beam is generated from a photoemission electron source (rf gun) and accelerated to $\sim$ 40 MeV in two superconducting cavities (CAV1 and CAV2). In this process, the operating parameters are tuned to minimize the transverse emittance [4]. In order to generate a low transverse emittance the charge density is reduced by illuminating the photocathode with a long laser pulse. The longitudinal emittance is increased when the beam is accelerated to its final energy due to quadratic correlations in the longitudinal phase space (LPS) imparted by the rf-wave curvature. To decrease the longitudinal emittance, a 3rd order accelerating cavity (CAV39) will subsequently be used. Before injection in the cryomodule, the bunch with appropriate LPS chirp can be longitudinally compressed using the magnetic bunch compressor (BC1) which consists of four 0.2-m rectangular dipoles (B1,B2,B3,B4) with bending angles of (+,-,+,-) 18°; see Fig. 1.

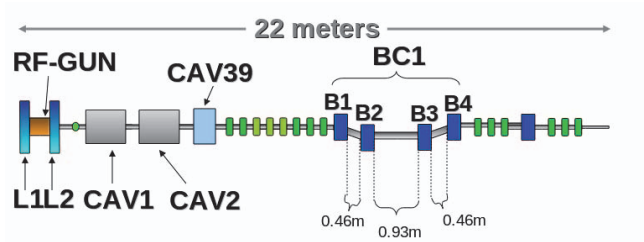

Figure 1: Overview of the ASTA photoinjector. The "RF-gun", "L1" and "L2" respectively correspond to the gun cavity and surrounding solenoid magnets, "CAV1", "CAV2" , and "CAV39" are superconducting rf cavities, "BC1" refers to the magnetic bunch compressor, and B1-4 are the dipoles of the chicane, with distance between the dipoles marked in the figure.

Two examples of LPS distribution simulated downstream of BC1 for an ideal compression, i.e. in absence of collective effects, appear in Fig. 2. The simulations carried out with ELEGANT [5] illustrate the benefits of the LPS linearization using CAV39 toward significantly improving the peak current. For these simulations, the LPS is modeled upstream of CAV2 with ASTRA as a 3.2-nC bunch, which is then loaded into ELEGANT. The linearization of the LPS is modeled with the transformation $\delta \rightarrow \delta_0 - bz_0^2$ where the parameter b is obtained from a polynomial fit of the incoming LPS distribution (z_0, δ_0).

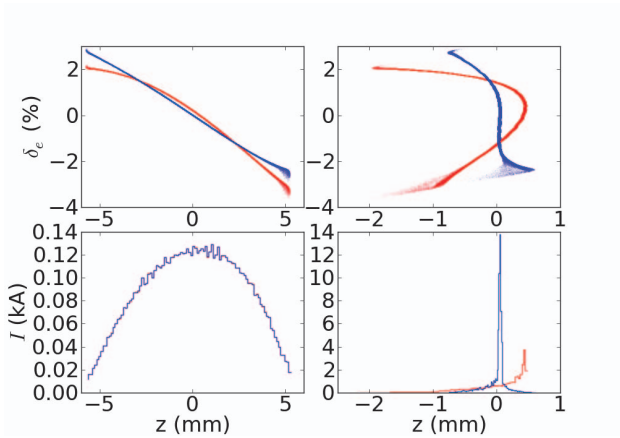

Figure 2: LPS distributions (top) and associated current profiles (bottom) before (left) and after (right) BC1. The red and blue traces correspond respectively to a linearized and nominal initial LPS.

*This work was supported by LANL Laboratory Directed Research and Development (LDRD) program, project 20110067DR and by the U.S. Department of Energy under Contract No. DE-FG02-08ER41532 with Northern Illinois University and under Contract No. DE-AC02-07CH11359 the Fermi Research Alliance, LLC.

COLLECTIVE EFFECTS

The simulation of collective effects along the photoinjector was, in our previous work [6], executed with IMPACT-Z [7]. The latter program includes a quasi-static 3-D space charge algorithm and a 1-D model of coherent synchrotron radiation (CSR). The CSR-induced energy loss is computed from the longitudinal charge distribution obtained from a longitudinal binning of the the macroparticle distribution. In this paper, we concentrate on the BC1 beamline and use the program CSRTRACK [8] which incorporates several models of the CSR integration, including a 3-D point-to-point (P2P) model. Since the P2P model is computer intensive (the calculation time scales as N^2 where N is the number of macroparticles), CSRTRACK also as an improved 1-D model referred to as projected (1DP) model, based on Ref. [9]. In CSRTRACK, the bunch is represented by an ensemble of macroparticles with charge distribution following a Gaussian distribution. Such representation is necessary to smooth the bunch charge distribution and reduce detrimental effects of numerical noise while allowing a decent representation of a bunch with has reduced number of macroparticles. The choice of the macroparticle size is a compromise between noise mitigation and the smearing of the bunch distribution's small-scale features. For the LPS distributions considered here, we typically found that a macroparticle size of 10% of the root-mean-square (rms) bunch length is appropriate [11].

In order to compare results of simulations performed with the different programs, we use the initial linearized LPS shown in Fig. 2 (b). The charge is set to 3.2-nC in order to consider a worst-case scenario. A scan of final parameters versus initial energy chirp $\mathcal{C} \equiv \langle z\delta \rangle / \langle z^2 \rangle$ appears in Fig. 3. The 1DP model of CSRTRACK is in good agreement with the IMPACT-Z including CSR effects only. However when SC effects are including in IMPACT-Z the emittance increases by 33%.

The simulation shown in Fig. 3 are performed for a nominal Courant-Snyder (C-S) parameter of $(\alpha_x, \beta_x) = (3, 8\ \mathrm{m})$, selected from the data displayed in Fig. 4. The latter Figure, generated with CSRTRACK's 1DP model, indicates loci of C-S couples that significantly mitigate emittance dilution during during the compression process. The area indicated by the black arrow corresponds to waists between B3 and B4, the location where the bunch is the shortest and CSR effects the strongest as discussed elsewhere [12]. The loci indicated by the red arrow corresponds to a waist between the B1 and B2 dipoles; see corresponding betatron functions for operating point (A) and (B) in Fig. 5. The solution (B) yields large betatron functions downstream of BC1 which render the lattice more susceptible to higher-order effects (e.g. chromatic aberrations).

Figures 6 and 7 show results of the 3D CSRTRACK simulations, and their comparison to the full IMPACT-Z models and the simpler CSRTRACK simulations. Table 1 compares the resulting emittances, energy spreads, and peak currents for the various simulations. Note that the simulations presented in this paper account for only the short distance of one meter after the last dipole of the chicane, while SC effects (and some tail of CSR that travels along with the bunch after the dipole) are of continuing detriment to the

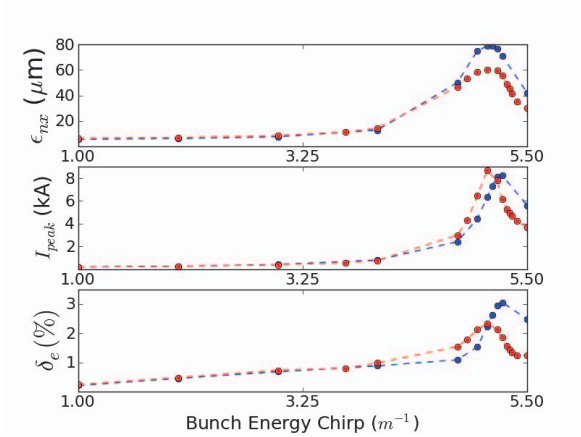

Figure 3: Final transverse emittance (left), peak current (middle), and energy spread (right) for a scan of Bunch Energy Chirp for three different types of simulations, with a LPS-linearized (to first-order) 3.2-nC bunch, with IMPACT-Z's SC+CSR model (blue) and CSTTRACK's Projected model (red).

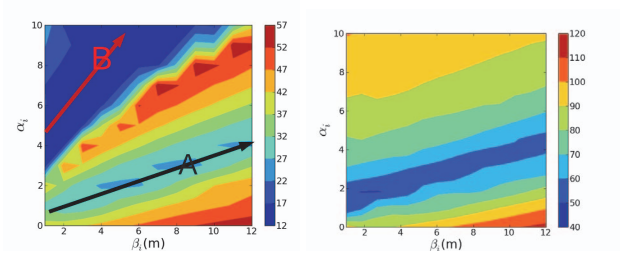

Figure 4: Contour plot of the final normalized horizontal emittance (ε_x in μm) a function of the initial C-S parameters for the nominal (left) and linearized (right) incoming LPS. The simulations are performed with CSRTRACK's 1DP model. The black arrow indicates a region where the beam reaches a waist between the 3rd and 4th dipoles, and the red arrow indicates where the beam reaches a waist between the 1st and 2nd dipoles.

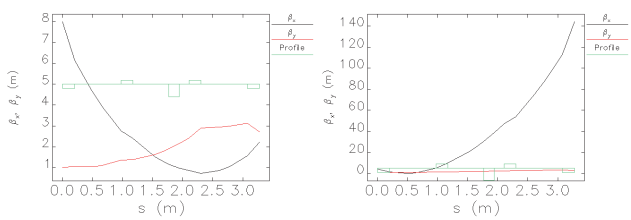

Figure 5: Betatron functions evolution along BC1 simulated with ELEGANT. The right and left plots correspond respectively to points (A) and (B) in Fig. 4.

ISBN 978-3-95450-115-1

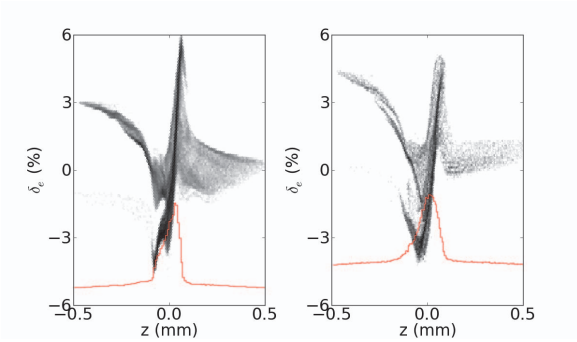

Figure 6: LPS at the end of the bunch compressor, with IMPACT-Z using 200k particles (left) and CSRTRACK's P2P model with 30k particles and 10% RMS sub-gaussians (right), for an initial chirp of 5.25m^{-1} and bunch charge of 3.2-nC.

phase space until it is accelerated in the first cryomodule.

Table 1: Simulated beam parameters downstream of BC1 with IMPACT-Z ("IMPZ") and CSRTRACK ("CSRT") the model used are appended to the program's name. "Par." is the parameter column and indicates the number of bins, or the absolute or relative (in %) Gaussian particle size.

Model	N	Par.	$\varepsilon_x(\mu\text{m})$	$\delta(\%)$	$\hat{I}$ (A)
IMPZ-1D	$2\cdot10^5$	256[a]	71.1	3.06	8.25
CSRT-1DP	$2\cdot10^5$	1 μm	55.4	1.85	6.16
CSRT-1DP	$2\cdot10^5$	10%	54.9	1.83	8.04
CSRT-1DP	$2\cdot10^5$	5%	54.5	1.87	8.78
CSRT-1DP	$2\cdot10^5$	1%	55.3	1.87	7.73
CSRT-P2P	$5\cdot10^3$	10%	101	2.81	6.37
CSRT-P2P [b]	$5\cdot10^3$	10%	103	3.03	6.65
CSRT-P2P	$1\cdot10^4$	10%	102	2.89	6.57
CSRT-P2P	$2\cdot10^4$	10%	94.6	2.91	6.44
CSRT-P2P	$3\cdot10^4$	10%	98.4	2.86	6.44
CSRT-P2P	$2\cdot10^4$	5%	97.8	2.80	5.95

[a] number of longitudinal bins; [b] a different statistical sample of the 2×10^5 particles was used compared to previous line.

VARIOUS BUNCH CHARGES

At ASTA, the bunch charge will be variable from a few pCs to several nCs. Some application, e.g. the test of ILC subsystem, call for a 3.2 nC, while other experiments, e.g. high-brilliance X-ray generation via channeling radiation, require very low charge. It is therefore of interest to assess the performance of the BC1 over the anticipated range in charge. Following Ref. [13], we introduce the transverse brightness $B_\perp=\frac{\hat{I}}{4\pi^2\epsilon_x\epsilon_y}$. Fig. 8 confirms that high charges results in lower value of $B_\perp$. At these charges operating the BC1 for maximum bunch compression results in a decrease of $B_\perp$ by one order of magnitude.

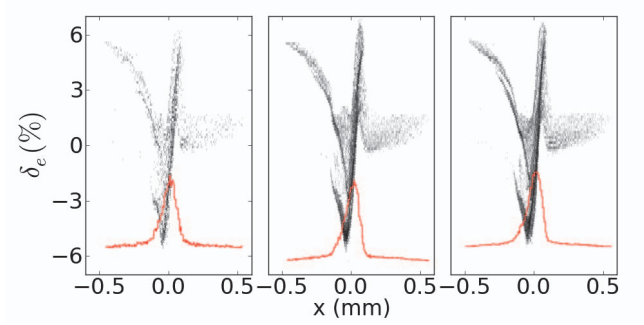

Figure 7: 3D model in CSRTRACK, with 5k (left), 20k (middle), and 30k (right) macroparticles randomly down-sampled from the same 200k particle distribution, with 10% sub-gaussians.

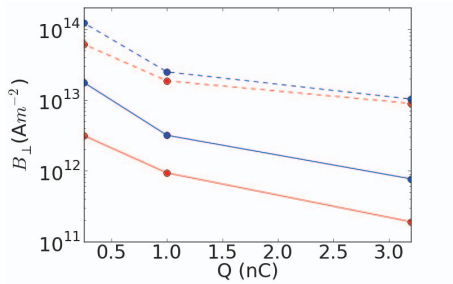

Figure 8: Transverse brightness $B_\perp=\frac{\hat{I}}{4\pi^2\epsilon_x\epsilon_y}$ versus bunch charge for IMPACT-Z's (red) and CSRTRACK's 1DP (blue) models. Dashed lines show each code's "ideal" case, using the final peak current but the initial emittances.

REFERENCES

[1] M. Church, et al, Proc. of PAC07, 2942 (2007).

[2] J. Leibfritz, et. al, Proc. of PAC11, MOP009 (2011).

[3] C. Prokop, et. al, FERMILAB-TM-2516-APC (2011).

[4] P. Piot, et al., Proc. of IPAC10, THPD020 (2010).

[5] M. Borland, Advanced Photon Source LS-287, September 2000 (unpublished).

[6] C.R. Prokop, et al., Proc. of PAC2011, p. 1561 (2011).

[7] Ji Qiang, et al., Journal of Computational Physics **163**, p. 434 (2000).

[8] M.D. Dohlus et al., Proc. of the 2004 FEL Conference, p. 18-21 (2004).

[9] E.L. Saldin, et. al, Nuclear Instruments and Methods in Physics Research **A 398** p. 373-394 (1997).

[10] B. Carlsten, et al., Physical Review E, Vol. 51 **2** p. 1453 (1995).

[11] C.R. Prokop, et. al, FNAL-TM-2533-APC.

[12] M. Dohlus, T. Limberg, in Proc. of PAC05, Knoxville, Tennessee, 1015-1017 (2005).

[13] B.J.Claessens, et al., PRL **95** 164801 (2005).